Direct laser writing lithography of photo-insensitive durable GST thin films with near 100% yield Supplementary Information

Roseanna G. Lawandi, Dylan J. Morden, Shiqi Luo, Shivashankar Vangala, Andrew M. Sarangan, Imad Agha

November 2024

S.1 Diffraction considerations

The beam waist of the focal spot for a beam much wider than the entrance pupil of a high numerical aperture objective is given by the diameter of the Airy Disk, $D=1.22\frac{\lambda}{NA}$, where λ is the wavelength of the beam, and NA is the numerical aperture from which the full-width at half-maximum (FWHM) can be calculated to be $0.42 \times D$.

In our experiments, we used a Gaussian beam illuminated through the lens aperture to avoid the loss of energy due to beam clipping. The beam waist at the focus is calculated by the formula $\omega = \frac{\lambda}{NA}$. From this, the FWHM of the Gaussian beam can be calculated as $\frac{1}{1.7}$ the beam waist. For the lens used in this experiment, with an NA of 1.3 under oil immersion, the theoretical beam FWHM is $\sim 240~nm$. Due to slight imperfections, our estimate on the beam size is around 270 nm, which is the basis of our numerical modeling.

S.2 Thermal limits on ultimate resolution

In order to crystallize a reasonably thick $Ge_2Sb_2Te_5$ (GST) sample from top to bottom using a laser, we can approximate the volumetric heat generation S as:

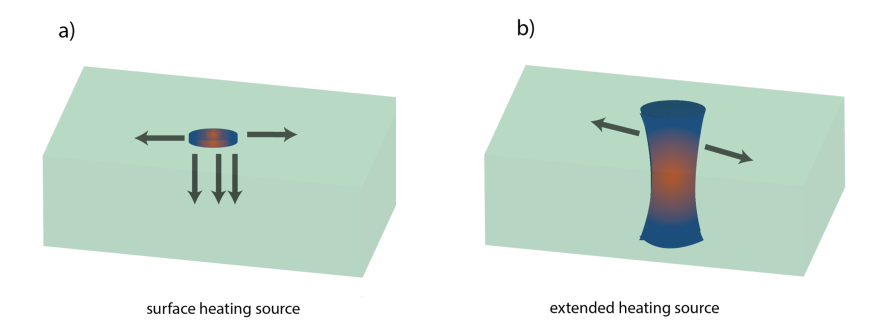
$$S = I_0 \delta e^{-\delta z} \tag{1}$$

where I_0 is the laser intensity, δ is the absorption coefficient, and z is the depth into the sample. When the sample is fairly transparent (e.g. using a 1064 nm laser on a 100 nm GST film), this allows the heat source to be approximated as a cylinder that extends from the top to the bottom of the film (Fig. S.1). On the other hand, for a shorter wavelength (e.g. 532 nm) where the absorption depth is ~ 10 nm, the laser-induced heating is confined to the top of the

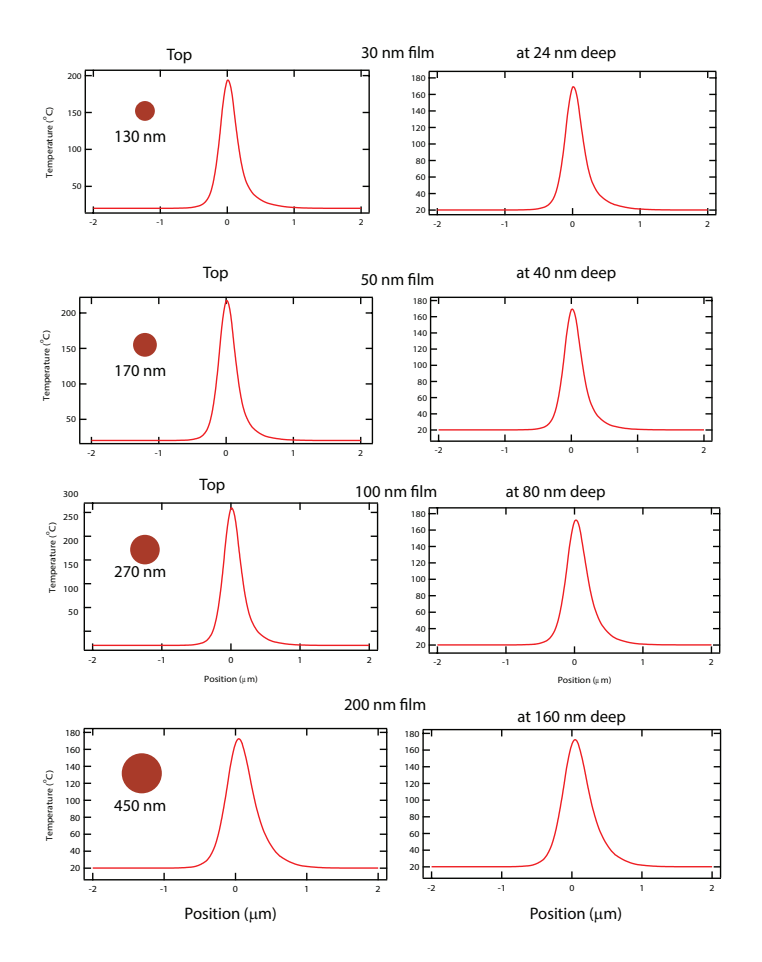
thin film, with isotropic thermal diffusion and crystallization wave propagation being the chief mechanism for fully crystallizing the film top to bottom, which inevitably leads to both lateral spreading of the crystallized area in addition to large vertical temperature gradients that may damage the film (e.g. when heated beyond the melting point).

While near-complete vertical crystallization may not be needed for certain applications, it is critical to photothermal lithography especially when dry etching is used to remove the "non-written" regions in a manner similar to positive photochemical resists. Since wet etching is isotropic, incomplete vertical crystallization leads to an undercut underneath the exposed region, which can fully lift-off any written feature when the etchant reaches the thin film below. A general rule of thumb is to prevent the undercut from exceeding $\sim 25\%$ of the spot size, which roughly requires the crystallization depth to be $\sim 80\%$ of the GST film thickness. This depth can be controlled either by increasing the peak power or the pulse length.

This and the information in section S.1 are the basis of our process optimization. A shorter wavelength is desired to achieve a smaller laser spot size on the sample, following the diffraction limit, however, that sets a limit on the film thickness that can be adequately crystallized before a) lateral diffusion makes the choice of a short wavelength laser less relevant, or b) temperature at the surface exceeds the melting/damage point of GST. On the other hand, the desired feature size and the etch selectivity of GST vs. the film to which the pattern is transferred, determine which GST thickness is ideal for the application at hand. Figure S.2 shows the profile of the crystallized spot at the film surface and at 80% deep, with both exceeding the threshold for phase transition. It is noted that, for 532 nm wavelength, a 200 nm film is the upper bound before melting occurs.



S. 1: a) Heat source in the high absorption, lower wavelength regime; absorption is confined to the surface. b) Heat source when the GST film is excited by a laser wavelength in the low absorption regime; the heat source should closely follow the focused Gaussian beam. Arrows indicate the directions of thermal diffusion (lateral or vertical).



S. 2: Temperature profiles and crystallization spot sizes at the top and near the bottom of the GST film for film thicknesses from 30 to 200 nm.

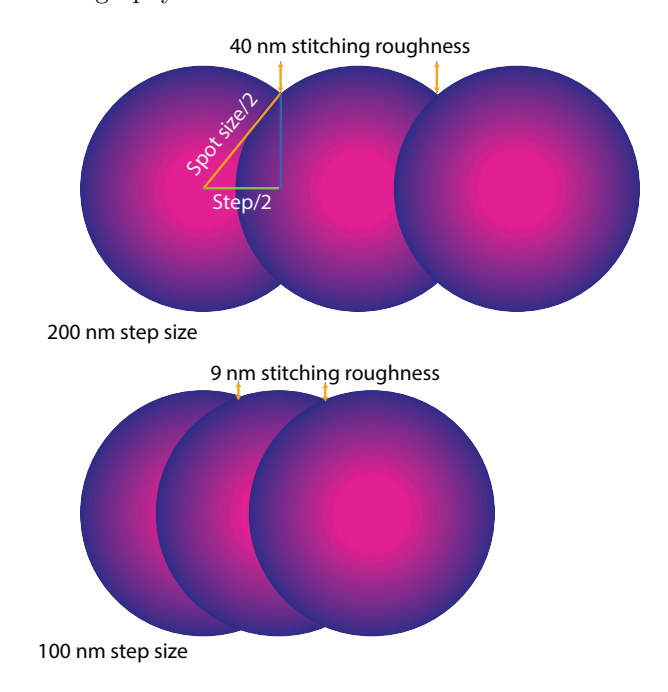
S.3 Effect of spot size and step size

The spot size associated with a single laser pulse-induced crystallization can be estimated from both the calculations in section S.2 as well as from the visual inspection under a high-magnification microscope. For 532 nm wavelength and 100 nm film, we estimate a single spot of around 250-270 nm. The pulse-step-pulse nature of direct laser writing is shown in Fig. S.3 for a 300 nm spot size beam with step sizes of 200 nm and 100 nm, respectively. Once a laser pulse hits the sample and crystallizes a spot, thermal relaxation on the order of a μ s occurs, after which the stage can be stepped before the onset of the next pulse. The interplay between step size and spot size leads to a stitching induced roughness (SR) that can be calculated as:

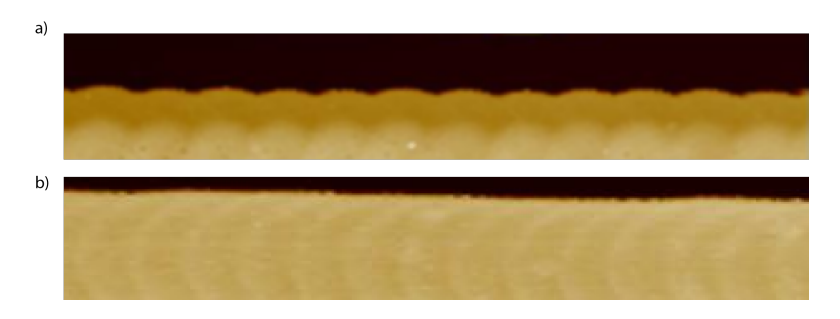
$$SR = \frac{1}{2}spot - \sqrt{\frac{1}{4}spot^2 - \frac{1}{4}step^2}$$
 (2)

where *spot* is the crystallized spot size and *step* is the step size.

Figure S.4 shows AFM images for a 900 nm spot size (achieved via a 4 μ s pulse) and both 400 nm and 200 nm step sizes, respectively. Theoretically, we expect roughness on the order of 47 nm and 12 nm, respectively. By analyzing the AFM images, we find the roughness to be 44.2 \pm 5.1 nm and 17.6 \pm 3.9 nm, respectively, which is in reasonable agreement with the theoretical calculations. This, additionally, indicates that the natural roughness due to the fundamental limits of GST lithography is well below 10 nm.



S. 3: Schematic showing the reduced sidewall roughness achievable by overlaying the crystallizing optical pulses.



S. 4: AFM images of a grating line written by stitching 900 nm spots with: a) 400 nm step size; b) 200 nm step size.

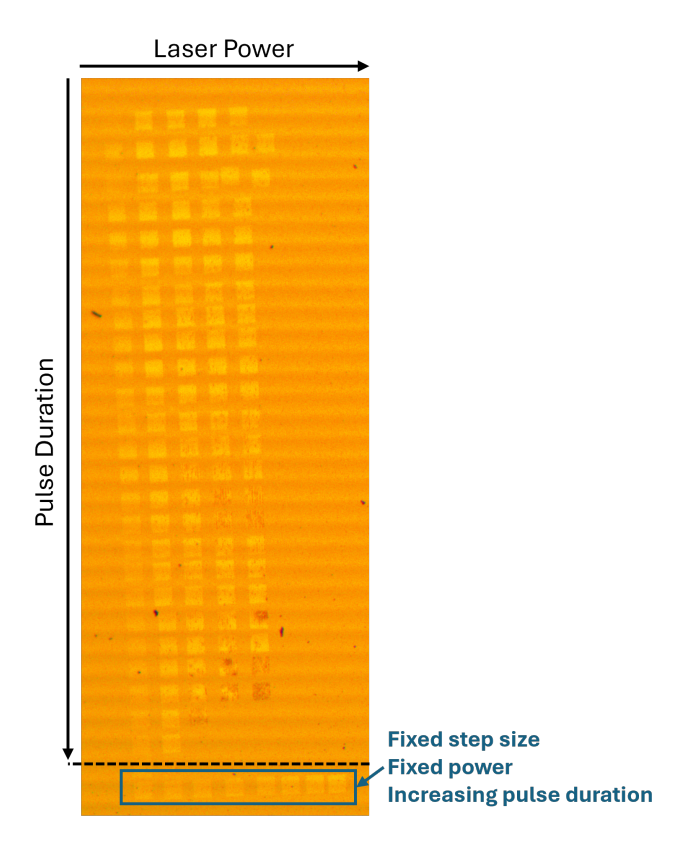
S.4 Effect of laser power and pulse duration

GST crystallization can occur over a broad range of temperatures, provided the threshold temperature of 175°C is exceeded. To optimize the patterning conditions, we conducted a detailed study on the effects of varying laser power and pulse duration. A matrix of gratings was patterned, with pulse duration increasing down the rows and laser power increasing across the columns (Fig. S.5). Additionally, we explored different pulse stepping strategies to minimize lateral thermal diffusion, which can degrade the fidelity of the grating features. At high laser power and long pulse durations (corresponding to the bottom right corner of the matrix), we observed ablation of the GST film, which led us to halt any further increase of these parameters.

In the final row of patterned features (identified by the blue box), the step size—defined as the distance between consecutive laser pulses—was kept constant at 1.5 μ m in the x-direction and 0.4 μ m in the y-direction and the laser power density was fixed at 5.9E+3 W/cm² to isolate the effect of pulse duration on feature survival. Within this row, only the pulse duration was varied, ranging from 4 μ s to 30 μ s, to investigate how extended heating times influence the size, shape, and quality of the resulting crystallized patterns. This allowed for a focused analysis of thermal accumulation effects and provided insight into the dynamics of the phase-change crystallization process under controlled conditions.

After completing both the wet and dry etching processes, the sample was examined using various optical characterization tools. To showcase the results, Fig. S.6 presents the SiO₂ grating matrix, combining the optical microscope image with selected high-quality SEM images highlighting successful patterning outcomes.

Since the power density of $5.9E+3~W/cm^2$ produced the most versatile results, yielding stable features across a broad range of pulse durations from 400 ns to 30 μ s, it was identified as the optimal setting for our application. For the pulse duration, the shortest duration that still produced survivable features was selected to minimize thermal diffusion and, consequently, maximize resolution.

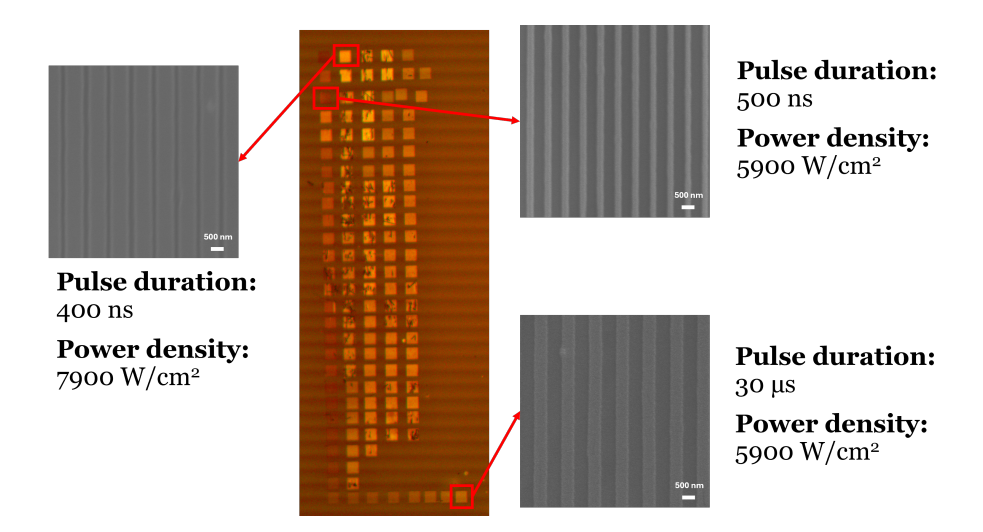


S. 5: A matrix of patterned GST gratings with pulse duration ranging from 400 ns to 4 μs and laser power density increasing from 5.9E+3 W/cm² to 10.6E+3 W/cm². In the final row of patterned features (marked with the blue box), the step size was held constant (x = 1.5 μm , y = 0.4 μm) along with a fixed power density of 5.9E+3 W/cm², while the pulse duration was varied from 4 μs to 30 μs .

Lastly, the optimal step size was determined based on AFM results, similar to those presented in Section S.3.

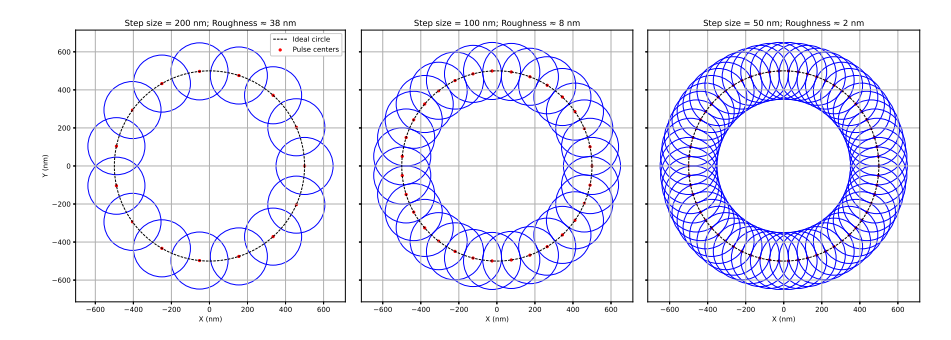
S.5 Limits of curved patterning

Using direct laser writing, curved patterning is easily implemented by adjusting the step size and direction between pulses. This can induce higher roughness on the feature sidewalls if the step size is not minimized. To illustrate the sidewall roughness and the curvature limits, a script is written to show the roughness limits for a 300 nm spot size. Figure S.7 shows the roughness achieved using the step sizes 200 nm, 100 nm, and 50 nm, while maintaining a fixed center radius



S. 6: Optical microscope image and selected SEM images of the ${\rm SiO_2}$ grating matrix after wet and dry etching, highlighting well-defined features, successful patterning results, and their corresponding laser parameters.

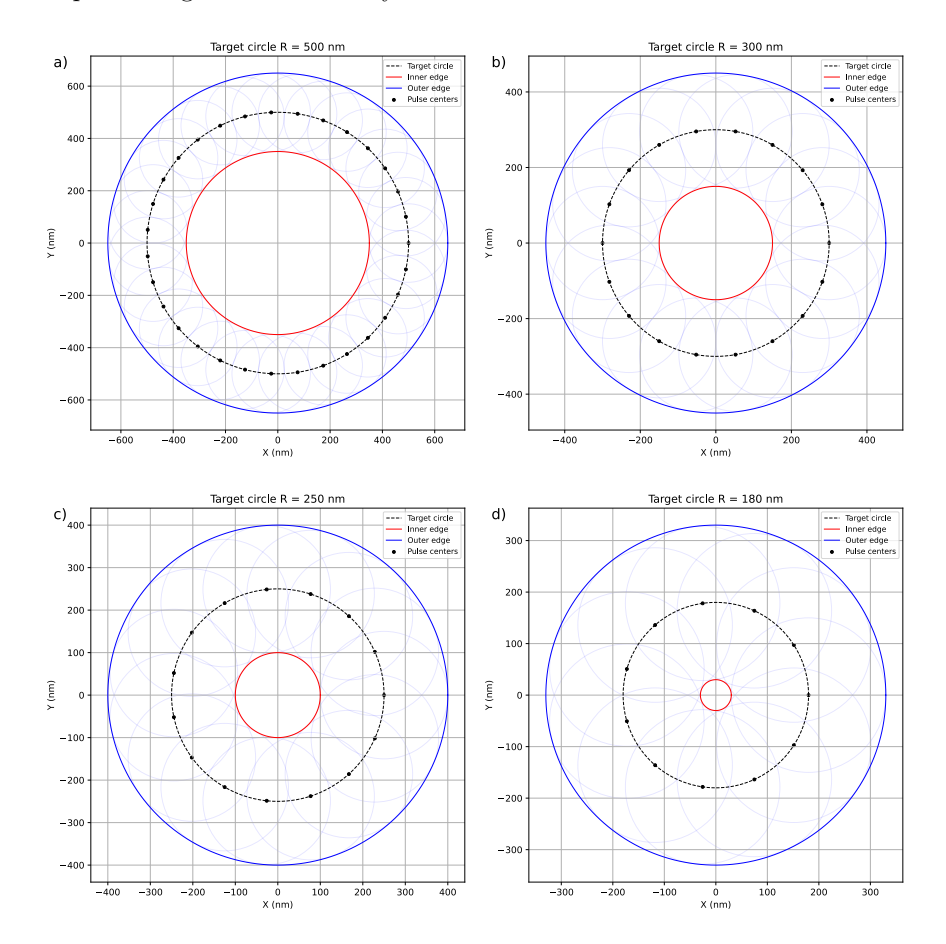
of curvature of 500 nm. As expected, a significant improvement in roughness is observed when the step size is reduced to 50 nm.



S. 7: An illustration of the reduction in stitching-induced roughness by decreasing the step size for a circular pattern with a 500 nm radius of curvature and a 300 nm spot size.

To further elaborate on the limits of curved patterning using our direct laser writing setup, we demonstrate the smallest achievable radius of an O-shaped structure using a laser pulse with a fixed 300 nm spot size and a 100 nm step size (Fig. S.8). The size of the O-shaped structure is constrained by the inner edge of the patterned feature (red circle). Theoretically, the minimum radius of the target/black circle, where the pulse centers are located, is half the spot size. However, due to the lateral thermal dissipation discussed in Section S.2, pulse

overlaying causes a broadening effect. As a result, the radius of the target circle cannot be smaller than the spot size, concluding that the limitation of curved nanopatterning is determined by the feature linewidth.



S. 8: A demonstration of patterned O-shaped structures with different target radii of curvature, R: a) 500 nm, b) 300 nm, c) 250 nm, and d) 180 nm. The spot size and step size are fixed at 300 nm and 100 nm, respectively. Contours defined by: Red line – inner edges; Blue line – outer edges; Black line – target circle where pulse centers are located.

S.6 Comparison of lithography technologies

The direct laser writing technique presented in this work falls short of the critical dimensions achievable by the state-of-the-art commercial lithography technologies. However, our proposed method offers a low-cost lithography solution with features that are highly attractive for applications such as MEMS fabrication,

automotive electronic devices, and semiconductor manufacturing. To highlight the advantages of this approach, a comparison table with other lithography systems is provided below, showcasing the distinct benefits of the proposed photothermal lithography technique.

Lithography Technique	Resolution	Critical Dimension	Patterning Fixture	Cost	Throughput	Material Compatibility
Photothermal Lithography	Medium to High	50 nm to 100 nm	Maskless	Low	Moderate to High	Works with various materials (ex: PCMs, polymers)
Nanoimprint Lithography	High	10 nm to 50 nm	Specialized molds or stamps	Moderate	High	Limited to materials compatible with mechanical stress (ex: polymers, metals)
Electron Beam Lithography	Very High	<10 nm	Maskless	High	Low	Limited to materials compatible with e-beam exposure (ex: resist materials)
Extreme Ultraviolet Lithography	Very High	7 nm to 20 nm	Reflective mask	Very High	High	Limited to materials compatible with EUV exposure (ex: resist materials)

S. 9: A comparison table of various lithography techniques and their characteristics.